ORNL/CP-96643

Invited Paper
To be published in Proc. of Summer School on Molecular Dynamics Simulation of Thin-Film Growth and Computational Physics, China Center for Advanced Science and Technology, Beijing, China, June 2– 5, 1997

"ELECTRIC GROWTH" OF METAL OVERLAYERS ON SEMICONDUCTOR SUBSTRATES

Zhenyu Zhang, Jun-Hyung Cho, Qian Niu, Chih-Kang Shih, and Zhigang Suo

SOLID STATE DIVISION
OAK RIDGE NATIONAL LABORATORY
Managed by
LOCKHEED MARTIN ENERGY RESEARCH CORP.
Under
Contract No. DE-AC05-96OR22464
With the
U. S. DEPARTMENT OF ENERGY
OAK RIDGE, TENNESSEE

February 1998

DISCLAIMER

DISCLAIMER

Portions of this document may be illegible in electronic image products. Images are produced from the best available original document.

To be published in Proc. of Summer School on
Molecular Dynamics Simulations of Thin-Film Growth and Computational Physics,
China Center of Advanced Science and Technology,
Beijing, China, June 2-5, 1997.
(invited paper)

"Electronic Growth" of Metal Overlayers on Semiconductor Substrates

Zhenyu Zhang and Jun-Hyung Cho
Solid State Division, Oak Ridge National Laboratory, Oak Ridge, Tennessee 37831-6032 and Department of Physics and Astronomy, University of Tennessee, Knoxville, Tennessee 37996

Qian Niu and Chih-Kang Shih
Department of Physics, University of Texas at Austin, Austin, Texas 78712

Zhigang Suo
Mechanical and Aerospace Engineering Department and Princeton Materials Institute, Princeton University, NJ 08544

In this article, we present the main results from our recent studies of metal overlayer growth on semiconductor substrates. We show that a variety of novel phenomena can exist in such systems, resulting from several competing interactions. The confined motion of the conduction electrons within the metal overlayer can mediate a surprisingly long-range repulsive force between the metal-semiconductor interface and the growth front, acting to stabilize the overlayer. Electron transfer from the overlayer to the substrate leads to an attractive force between the two interfaces, acting to destabilize the overlayer. Interface-induced Friedel oscillations in electron density can further impose an oscillatory modulation onto the two previous interactions. These three competing factors, of all electronic nature, can make a flat metal overlayer critically, marginally, or magically stable, or totally unstable against roughening. We further show that, for many systems, these electronic effects can easily win over the effect of stress. First-principles studies of a few representative systems support the main features of the present "electronic growth" concept.

1 Introduction

For important scientific and technological reasons, it is desirable to grow metal thin films with atomically flat interface and growth front [1]. This has not been possible in many heteroepitaxial systems, however, because of fundamental obstacles such as stress effects [2,3,4] and kinetic limitations [5,6]. It has been a major focus of intensive studies to identify and overcome such obstacles in the quest for technologically important overlayers.

One example is the growth of Ag on GaAs(110), where a rough surface would results in typical growth conditions[7]. However, by using a two-step process (low-temperature deposition followed by room-temperature annealing), Smith *et al.* [8] were able to obtain atomically flat silver films. One startling observation was the existence of a critical thickness: A flat silver overlayer can be formed only if the total Ag coverage deposited exceeds a minimum value of about 15 Å. Similar observations have also been confirmed independently for the same system [9], and on two other III-V semiconductors, GaP(110) and GaSb(110) [10]. The underlining physical reason for the success of this approach is not known to date, and it is unlikely due to stress effect, because one should then expect exactly the opposite behavior: A flat film becomes unstable at sufficiently large thickness, where the adsorbed material tend to form three-dimensional islands or cracks to release the strain energy [2,3,4].

In a recent study, we developed what we termed the "electronic growth" model for formation of metallic overlayers on semiconductor substrates [11]. Unlike commonly rec-

ognized growth mechanisms based on considerations of stress effects [2,3,4] or kinetics of individual atoms [5,6], we placed primary emphasis on the energetics of the conduction electrons which are extended throughout a metal overlayer. Earlier studies have established that the electronic states within an ultrathin metallic overlayer can be quantized due to confinement in the direction of film thickness [12,13]. For metal overlayers on semiconductor substrates, we showed that these discrete electronic levels can play a crucial role in defining the overall stability of the overlayers. Depending on a delicate energy balance between an energy loss due to confinement and a gain due to charge spilling from the film to the substrate, the overlayer can be either stable above a critical thickness of typically a few monolayers (ML), or unstable for any thickness greater than 1 ML. For those systems in which the interface-induced Friedel oscillations in electron density within the overlayer are sufficiently strong, additional magic thicknesses for stable film growth can be defined. Our theory not only confirms the existence of the critical thickness for Ag growth on GaAs [8,9], but also explains the well-known fact that only the first layer of alkali metals can be smooth on semiconductors [14]. It further points to new directions for achieving smooth growth in many other systems where magic thicknesses may exist.

The paper is organized as follows. In Sec. 2 we present the simple phenomenological model used to convey the main ideas of the electronic growth concept, as well as the application of the concept to the growth of metals belonging to several different columns of the periodic table [11]. In Sec. 3, we compare directly the relative importance of these purely electronic effects with stress effects, and show that, contrary to traditional belief, the electronic effects can easily win over stress effects in stabilizing ultrathin films on semiconductors. We also derive the asymptotic form of the effective repulsive potential between the metal-semiconductor interface and the growth front, mediated by the conduction electrons [15]. In Sec. 4 we present a first-principles study of a model metal/semiconductor system, Sb/GaAs(110), showing that the main features of the electronic growth concept persist to show up in several dramatic ways [16]. Finally in Sec. 5 we summarize the main findings, together with a brief discussion of the application of the electronic growth concept to the formation of two-dimensional metal islands on surfaces [17].

2 The "Electronic Growth" model and its applications

We present our theory within the framework of a general thermodynamic stability analysis, which in spirit is similar to the shell model for the existence of magic atomic numbers in metallic clusters [18]. Let $U_t(L)$ be the total energy of the system with a flat film of thickness L. $U_t(L)$ also plays the role of the Hemholtz free energy at low temperatures. The film is stable if the "compressibility" is positive, i.e., $\partial^2 U_t(L)/\partial L^2 \geq 0$. Under this condition, any small roughness in the film tends to be suppressed when sufficient atomic mobility is provided. The film is unstable if $\partial^2 U_t(L)/\partial L^2 < 0$. In this case, the system can achieve a lower total-energy state by developing a mixed phase of different film thicknesses. A critical thickness, L_c, can be defined if the film is stable for $L \geq L_c$ but unstable for $L < L_c$ (or the other way around). Furthermore, a magic thickness, L_m, can be defined if $U_t(L)$ has a downward cusp at L_m, namely, the film is unstable on both sides of L_m. Our main task is to show when and why there can exist critical and

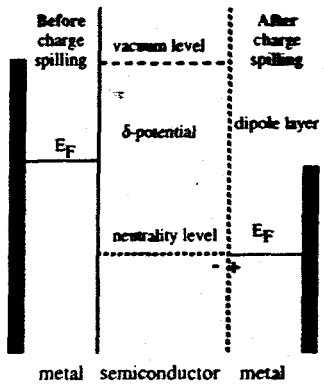

Figure 1: Schematic energy diagrams of a metal-semiconductor interface before charge spilling (the left two panels), showing the relatively high Fermi level of the electrons in the metal film; and after charge spilling (the right two panels), showing the alignment of the Fermi levels and the establishment of a dipole layer.

magic thicknesses in the formation of metal overlayers.

The energy of the system can be evaluated by referring to the ideal situation where the film is isolated from the semiconductor substrate, with charge neutrality maintained on both sides of the interface, and with the interface atoms neither reconstructed nor relaxed. The energy of the actual system, U_t, is then estimated as $U_t = U_0 - U_c$, where U_0 is the energy of the film in the ideal situation, and U_c is the energy decrease due to charge spilling as the delta potential is lowered. Figure 1 illustrates the band diagrams before and after charge spilling takes place. The vacuum levels of the film and the substrate should be equal before charge spilling. The Fermi energy and the energy of the film $U_0(L)$ in the ideal situation are estimated by a model of a free electron gas confined by a barrier step $(W_m + E_F)$ on the outer surface and by an infinite hard wall at the interface, where W_m and E_F are the work function and Fermi energy (relative to the bottom of the conduction band) of the metal in bulk form. After subtracting a term linear in the film thickness, which does not change the conclusion about film stability, the function $U_0(L)$ curves up as the film thickness becomes small, a quantum-size effect in the film thickness direction (see Fig. 2).

The Fermi energy of the semiconductor substrate is taken to be at the charge neutrality level in the gap [19]. Once the Fermi level difference ΔE_F between the metal film and the substrate is calculated in the ideal situation, the energy lowering due to charge spilling can be expressed as $U_c = 0.5C(\Delta E_F/e)^2$, where e is the electron charge, $C = \varepsilon_0/(\ell_m + \ell_s/\kappa)$ is the interface capacitance, ε_0 is the vacuum dielectric constant, ℓ_m and ℓ_s are the length scales for charge redistribution on the metal and semiconductor side of the interface, respectively, and $\kappa \approx 2$ is the effective dielectric constant of the semiconductor near the interface [20]. The length scale for charge redistribution on the metal side can be estimated by the Thomas-Fermi screening length (0.59 Å for Ag) [21], while the length scale on the semiconductor side is taken as the tunneling distance at the charge neutrality level (about 2.8 Å for GaAs) [22]. The resulting energy lowering U_c

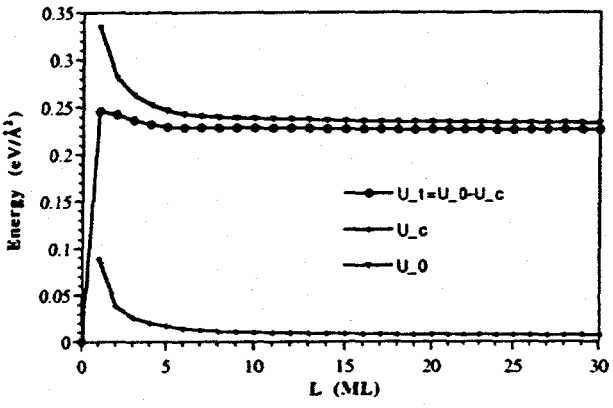

Figure 2: Film thickness dependence of the film energies for Ag on GaAs(110). The cusp-like feature at L= 5 ML defines the critical thickness for flat film growth.

also curves up as the thickness becomes small, because the Fermi energy of the film is squeezed higher by the quantum confinement (see Fig. 2).

The total energy $U_t = U_0 - U_c$ for Ag/GaAs(110). shown in Fig. 2, has a shape predicting the existence of a critical thickness. The energy lowering due to charge spilling has a steeper thickness dependence at smaller L, pulling the total-energy curve down. This makes the curvature of $U_t(L)$ negative in that region, rendering flat films unstable. The curvature changes sign at $L = 3$ ML, and has a cusp-like dip at $L = 5$ ML, indicating that a flat film at this thickness is particularly stable. This cusp is mainly caused by the sharp energy features of the quantum well states and the Fermi surface. The curve is practically flat beyond $L = 5$ ML, showing that thicker flat films are all marginally stable. We therefore identify $L_c = 5$ ML as the critical thickness, which is of the same magnitude as the experimental finding of $L_{c,expt} \sim 7$ ML [8,9]. The agreement is satisfactory, considering the fact that the simple model does not contain any adjustable parameters, and that there is some uncertainty in the determination of the absolute coverage of the film in the experiments [8,9]. Finally, we notice that if we follow Ref. 23 by using the empirical formula $\kappa = (1 + \kappa_s)/2 = 7$, where $\kappa_s = 13$ is the dielectric constant in bulk GaAs, then the enhanced energy lowering due to charge transfer would cause the change of curvature right at $L_c = 5$ ML.

The above calculations can be easily repeated for other metal-substrate systems. In these calculations, we assume that the metallic overlayer always prefers to grow in close-packed forms in the film thickness direction, as is the case for Ag [8,9,10]. Here we limit our discussions to different metals on the same GaAs(110) substrate, with detailed comparisons of the effects of different substrates presented elsewhere [10]. The stabiliy of Cu and Au films resembles very closely that of Ag, each with the same critical thickness of ~ 5 ML. This type of stability of an ultrathin metallic film is reproduced and designated as Type A in Fig. 3. In contrast. a qualitatively different type (Type B) is obtained for the alkali metals (Li, Na, K, Rb, and Cs), as represented by the case of Na in Fig. 3. Here, because of its small work function, the energy gain due to charge spilling dominates, leading to downward curving in U_t, with $\partial^2 U_t(L)/\partial L^2 < 0$. Therefore, a flat

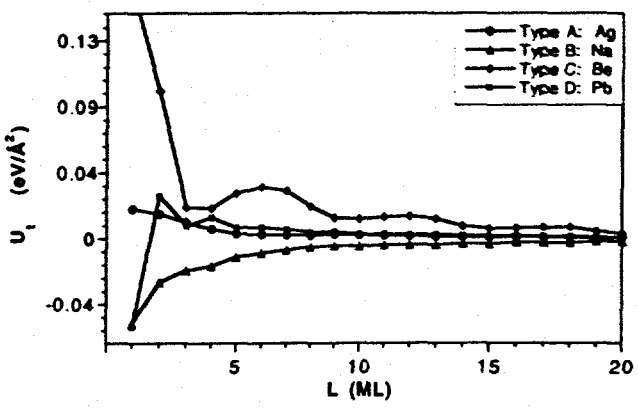

Figure 3: Comparison of four representative types of film stability for different metals on GaAs, as defined in the text. Notice that an element-specific constant term has been subtracted from each curve to make the total energy equal to zero at large film thickness.

film thicker than 1 ML is unstable, because it is always possible to reduce its energy by phase separating into a rough film with smaller and larger thicknesses. This explains the well known experimental fact that one cannot grow a smooth film of alkali metals of more than 1 ML on GaAs(110)[14].

We have also investigated the quantum-size effects for overlayer growth of alkaline earth metals (Be, Mg, Ca, Sr, and Ba). Unlike the alkali metals which qualitatively all follow the same curve (Type B in Fig. 3), the alkaline earth metals have very different behaviors among themselves. Ca, Sr, and Ba are similar to the alkali metals (Type B), but Be and Mg belong to a new type (Type C), as represented by the case of Be in Fig. 3. Here, the film is magically stable around $L_m = 3$ ML; furthermore, there still exists a critical thickness at $L_c = 9$ ML above which the film is marginally stable. Calculations show that Zn and Cd also belong to Type C.

A fourth type of behavior is shown as Type D in Fig. 3, followed by both Al and Pb on GaAs. Here, the energy dependence is a damped oscillatory one, with a period of oscillation equal to 2 ML. Such oscillatory behaviors have been predicted in earlier studies of quantum-size effects in metal/metal systems[13].

The oscillatory thickness dependence of $U_t(L)$ for Types C and D is caused by the interface-induced Friedel oscillations. To illustrate this, it is sufficient to plot in Fig. 4 the density of a semi-infinite electron gas confined by a hard wall (the interface):

$$\rho(u)/\rho_0 = 1 + 3[\cos(u) - \sin(u)/u]/u^2, \qquad (1)$$

where $u = 2k_F z$, z is the distance from the interface, and k_F is the Fermi wave vector[21]. For a given metal (characterized by its own k_F and interlayer spacing, d), the electron density at different layer thicknesses ($z = Ld$, with $L = 1,2,3\ldots$) sample different points on the same curve. If a given film thickness coincides with a minimum of the Friedel oscillations, then there is an additional energy gain, because fewer electrons need to be pushed up in energy by the confinement of the outer surface. For Na and Ag, the first (and also the deepest) minimum in the density oscillations located between 3 and 4 ML

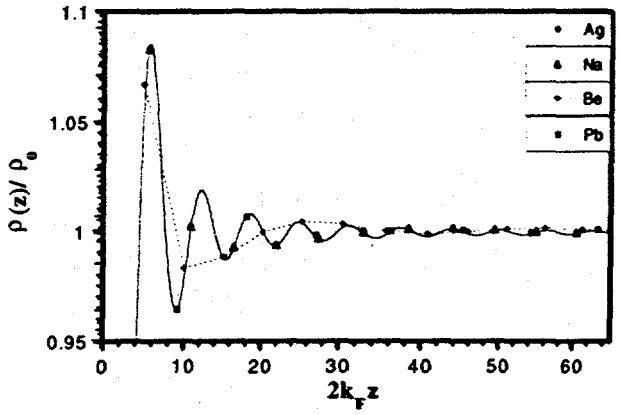

Figure 4: Friedel oscillations in electron density within a semi-infinite metal caused by a hard wall located at the metal-semiconductor interface. The different metal elements sample different sets of points on the same curve.

is too shallow to induce an additional magic thickness. In contrast, the first minimum for Be is large, which results in the existence of a magic thickness. For Pb, the position of the first minimum located at 1 ML coincides with the first minimum of the universal Friedel oscillation curve; this perfect phase matching in the Friedel oscillations and that due to lattice periodicity explains why, as seen in Fig. 3. the total energy at $L = 1$ ML is so low for Pb.

The above semi-quantitative analysis has demonstrated a very plausible and important concept in film growth, that the electronic energy of an ultrathin metallic overlayer can play a crucial role in determining the overall stability of the overlayer and the morphological evolution during its growth. The three central and competing components of the theory, namely, the quantization of the electronic states. the charge spilling. and the Friedel oscillations. should show up in any reasonably accurate treatment of the problem. In contrast, some earlier treatments of the problem using free-standing films would miss the important effects due to charge transfer [13], without which it would be impossible to define the critical thickness for Ag/GaAs or to explain why only the first layer of an alkali metal can be grown smoothly. Also, the essential predictions of the present theory remain valid if all other factors can only give rise to a smooth modification to the total-energy curve, including possible shifts in the locations of the critical/magic thicknesses. What remains to be explored is how the electronic effects discussed here compete with stress effects, the subject of the next section.

3 Direct comparison between the quantum size effects and stress effects

An epitaxial film on a substrate of a different material is often under stress. The elastic energy may motivate atoms to diffuse on the surface and change the film morphology. Experimentally it has been known that whether a film remains flat or forms islands depends on its thickness. On a Si substrate, for example, a flat Ge film is stable up to three monolayers; above this thickness, islands form [24]. Similar behavior, sometimes with thicker wetting layers, has been reported for some other inorganic and organic semi-

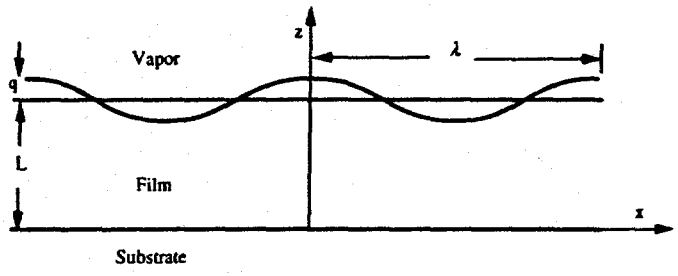

Figure 5: An epitaxial film on a substrate. The film surface is perturbed into a wavy shape of wavelength l and amplitude q.

conductor films[25]. The recent observation of the inverse critical thicknesses for smooth growth on Ag on III-V semiconductors adds another kind of thickness dependence for metallic films[8,9,10]. In the previous section, we showed that the long-ranged interactions associated with the electronic energy of a metallic overlayer can lead to various types of thickness dependence. In this section, we consider explicitly the competitions between surface tension, stress, and effective long-ranged forces mediated by the conduction electrons, and show that the latter can win over stress in stabilizing metal films of many monolayers[15].

Before introducing long-range force effects, we recall that the existing model addressing the stability of epitaxial films invokes surface tension and elasticity[3,26]. Figure 5 illustrates a film of thickness L on a semi-infinite substrate. The surface tension of the film, γ, is taken to be isotropic[27]. The stress in the film, σ, results from the difference of the film and the substrate in, for example, crystal structure, lattice constant or thermal expansion coefficient. When the surface is flat, the stress is uniform in the film. Consider a two-dimensional problem, representing the substrate by a semi-infinite plane, and the film by an overlaying strip; atoms can diffuse along the curve representing the film surface. The model is based on a stability analysis. Atomic diffusion on the surface conserves the mass of the film. Consequently, one can perturb the surface into a wavy shape above and below the average film thickness, L, namely,

$$z = L + q\cos(2\pi x/\lambda) \tag{2}$$

where z is the perturbed film thickness, q the wave amplitude, and λ the wavelength. The x-axis coincides with the film-substrate interface.

To highlight the thermodynamic nature of this instability, we focus on energetics and avoid details of the mass transport process. All energies are computed for one period of the system, per unit thickness in the direction normal to the plane, to the leading order in the perturbation amplitude q. The surface energy, U_S, is γ times the length of the curve that represents the surface. One can readily show that the perturbation increases the surface energy by

$$\Delta U_S = \pi^2\gamma q^2/\lambda \tag{3}$$

Elementary considerations dictate that, when the surface undulates, the elastic energy stored in the system, U_E, should decrease, and its change should take the form

$$\Delta U_E = -\beta\sigma^2 q^2 / Y \tag{4}$$

Here Y is Young's modulus of the film, and β a positive dimensionless number, which has been calculated by solving the boundary value problem of a strained, perturbed film on a substrate [3,25]. If the film and the substrate have identical elastic constants, $\beta = \pi$. The total free energy, $U_S + U_E$, increases for short wavelengths, but decreases for long wavelengths. Consequently, the flat film of any thickness is unstable. For the film and the substrate having different elastic constants, β depends on λ/L and ratios of the elastic constants. Nonetheless the conclusion remains essentially unchanged: except for a film on a rigid substrate, the stressed film of any thickness is unstable.

This conclusion clearly disagrees with experimental observations cited in the beginning of this section. One may settle with the thought that the continuum model fails for thin films. On the other hand, thickness effects of various kinds have been observed in many systems, some of which have stable films of many monolayers [8,9,10,25]. Consequently, it is imperative to have a model with a wider applicability.

In a recent study, we have proposed to include additional thermodynamic forces acting over longer ranges than atomic length [15]. In the presence of a long-ranged force, the change in the interaction energy associated with the surface undulation is

$$\Delta U_L = \int_0^\lambda U(z)\, dx - U(L)\lambda \tag{5}$$

This expression is reasonable when the wavelength of the perturbation is larger than the film thickness, and the amplitude of the perturbation is small. To the leading order in q, the change is

$$\Delta U_L = \frac{\lambda}{4}\frac{\partial^2 U}{\partial L^2} q^2 \tag{6}$$

As described in Sec. 2, when the function $U(L)$ is concave up, i.e., $\partial^2 U/\partial L^2 > 0$, the long-range force tends to stabilize a flat film. When $\partial^2 U/\partial L^2 < 0$, the long-range force tends to destabilize the flat film.

Observe from (3), (4) and (6) that the surface tension is effective in stabilizing the film against perturbations of short wavelengths, the long range interaction (assuming $\partial^2 U/\partial L^2 > 0$) is effective in stabilizing the film against perturbations of long wavelengths, and the stress destabilizes the film for all wavelengths. Summing up (3), (4) and (6) leads to the conclusion that the net free energy increases for perturbations of all wavelengths only if

$$\partial^2 U/\partial L^2 > \sigma^4/Y^2\gamma \tag{7}$$

This establishes the condition under which the flat film is stable against any small perturbation. (We have taken $\beta = \pi$ because elastic constants are often not too dissimilar between the film and substrate.) An analogous condition has been derived under the assumption that the film surface tension is influenced by the presence of the substrate [28].

Because no physical origin of such dependence has been specified. to the best of our knowledge, it has never been established so far that a long-range force, of any kind, is strong enough to stabilize a film against stress.

In Ref. 15, we applied (7) to the case of dispersion forces and showed that even the van der Waals forces can be strong enough to stabilize films of a few monolayers. Here we focus on the long-ranged forces associated with the confined electrons in metal films. As discussed in Sec. 2, a recent model has highlighted forces of two origins: quantum confinement and charge transfer [11]. In a metallic film electronic states form discrete subbands [12,13]. Consequently, if insulated, the film has higher average electronic energy than the bulk. This difference results in an excess free energy of the film relative to the bulk. (As an approximation, ions in the film and in the bulk are taken to have identical free energy.) On the other hand, when the metallic film is brought in contact with a semiconductor substrate, electrons transfer between the two media to equalize the Fermi level. This lowers the free energy. For Ag on GaAs, the calculations given in Sec. 2 showed that the attraction due to charge transfer dominates for very thin films. and the repulsion due to quantum confinement dominates for thick films. Fig. 6 shows the qualitative shape of the combined interaction energy. U. The curve is concave down for thin films, but concave up for thick films; the small circle on the curve marks the inflection point, corresponding to the film thickness L_0. which is about a few monolayers. As pointed out in Sec. 2. if the effect of stress is negligible. such a long range interaction destabilizes a film thinner than L_0, but stabilizes a film thicker than L_0. This trend agrees with the experimental observations [8,9].

We now include the effects of the stress and surface tension. The bottom part of Fig. 6 shows the shape of $\partial^2 U/\partial L^2$ as a function of L. The quantity $\sigma^4/\gamma Y^2$ is a horizontal line. According to the stability condition (7). three situations exist. (a) When the horizontal line is too high to intersect with the curve. the flat film is unstable for any thickness. (b) When the horizontal line is tangent to the curve, the flat film is stable only for one particular thickness, and unstable for any other thicknesses. (c) When the horizontal line intersects with the curve at two points. corresponding to films of thickness L_1 and L_2, the flat film is stable if its thickness falls in between. Using $\gamma = 1$ J/m^2. $Y = 76$ GPa, and $\sigma = 500$ MPa (a relatively large stress in metallic films), we obtain $\sigma^4/\gamma Y^2 = 10^{13}$ J/m^4. Our calculations, including both quantum confinement and charge transfer, with either finite or infinite potential well, gave the magnitude of the maximum curvature, $(\partial^2 U/\partial L^2)_{\max} = 10^{18}$ J/m^4. Note the huge difference between $\sigma^4/\gamma Y^2$ and $(\partial^2 U/\partial L^2)_{\max}$. Consequently, when the film is not too thick, the quantum confinement effect prevails over the stress by a large margin. Situation (c) is readily accessible experimentally: very thin films are destabilized by charge transfer, films of intermediate thickness are stabilized by quantum confinement, and thick films are destabilized by stress.

Because $(\partial^2 U/\partial L^2)_{\max} \gg \gamma Y^2$, from Fig. 6 we see that $L_1 \approx L_0$. However, L_2 must be estimated by using the long-range tail of the interaction energy. Everything else being equal, better confinement of electrons can stabilize thicker films. As an estimate of the magnitude of the long-range tail, consider electrons confined in a metallic film by infinite potentials on both sides. The energy levels are determined by the one-electron Schrödinger equation. The total free energy is estimated by the sum of energies over all electrons in the ground state of the film. As above, let $U(L)$ be the excess energy per

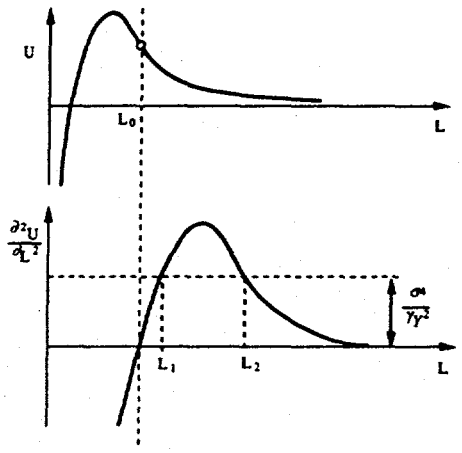

Figure 6: The top figure shows the qualitative shape of the function $U(L)$ for Ag on GaAs, where the inflection point is marked by a small circle. The bottom figure shows the qualitative shape of the curvature.

unit area of the film relative to that of the bulk of the same thickness. Our analysis shows a surprisingly long ranging tail:

$$U(L) = \frac{3\pi^2\hbar^2\rho}{32mL} \equiv \frac{B}{L} \tag{8}$$

where $\hbar$ is the Planck constant, m the electron mass, and ρ the number of free electrons per unit volume. Figure 7 compares this asymptotic result with the exact numerical solution; they agree well beyond a few monolayers. A combination of (7) and (9) gives

$$D_2 = \left(2B\gamma Y^2/\sigma^4\right)^{1/3} \tag{9}$$

For Ag, $n = 5.86 \times 10^{28}$ m^{-3} and $B = 6.62 \times 10^{-10}$ J/m. A stress of magnitude $\sigma = 500$ MPa leads to $L_2 = 496$ Å. The available experimental data do not permit a meaningful comparison. Equation (9) ignores fine oscillations that are invisible on the scale of Fig. 7. For finite confinement potentials, our numerical calculation shows that the interaction energies due to quantum confinement and charge transfer each has the $1/L$ tail, but with different proportionality constants. Consequently, these details do not change the qualitative behaviors at large L.

Our model predicts that the critical film thickness sensitively depends on the stress. This fact can be readily exploited in experiments. For example, the stresses in $In_xGa_{1-x}As$ films on a GaAs substrate depend on the composition x; the wetting layer thickness is known to be a strong function of the composition[29]. For a metallic film on a semiconductor substrate, thermal expansion misfit is large; for Ag on GaAs a temperature change can cause a stress change by 1.4 MPa/K. One expects that the critical thickness can be tuned by changing the temperature, as suggested in some experiments[9,25,30].

We are unaware of any experimental measurements of the long-range forces in crystalline films. The excess free energy U gives rise to a chemical potential of a thin film relative to the bulk:

$$\mu = \Omega\partial U/\partial L \tag{10}$$

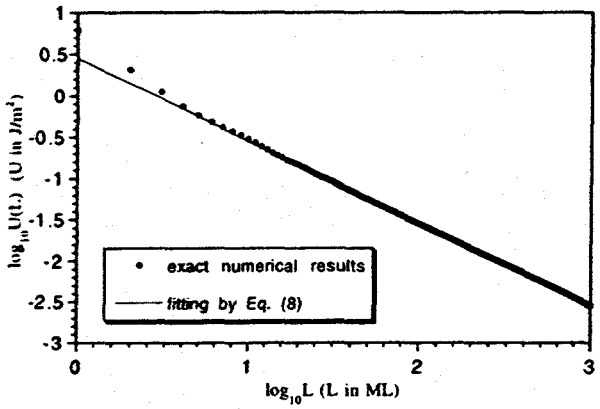

Figure 7: Comparison between the asymptotic long-range tail with numerical results, for a silver film confined by infinite potential on both sides.

where Ω is the volume per atom. Note that this chemical potential depends on the film thickness. It may be measured by suitable mass transfer experiments.

4 First-principles studies of a model system: Sb/GaAs(110)

So far all the discussions have been based on simple phenomenological models. The physical phenomena derived are novel and interesting, but will they survive if the systems are described by more rigorous, first-principles based interaction potentials? In this section, we present the results from a recent first-principles study of a representative system, Sb growth on GaAs(110) [16], in which we confirm many of the essential features derived using simple models.

As a prototype nondisruptive metal-semiconductor interface system, the growth of Sb on GaAs(110) has been investigated extensively [31,32,33,34,35,36,37]. Based on Auger electron spectroscopy [31] and scanning tunneling microscopy (STM) studies [32,33], the growth pattern of Sb has been found to follow a $(1+M)$ mode (or a modified Stranski-Krastonov mode): a monolayer followed by sets of multilayers of a well-defined thickness M (see Fig. 8). Moreover, $I-V$ measurements showed that the band gap at the Fermi energy decreases with increasing film thickness, suggesting a nonmetal-metal transition at a higher coverage [33]. Theoretically, most previous studies have concentrated on the adsorption of 1-ML Sb on GaAs(110) [34,35,36,37]. Our recent study this system in the multilayer regime aimed to provide the physical insights into the understanding of those growth phenomena.

In our study, the effects of quantum confinement and charge spilling are treated self-consistently, with inclusion of surface relaxation. We find strong manifestations of quantum size effects, in both known and unexpected ways. As the film thickness increases, the adsorption energy per layer oscillates, thereby defining the existence of magic thicknesses for smooth growth. This finding provides the microscopic basis for the $(1+M)$ growth mode. Furthermore, there exist corresponding oscillatory nonmetal-metal transitions, a surprising finding in contradiction with traditional belief. We will identify the underlying

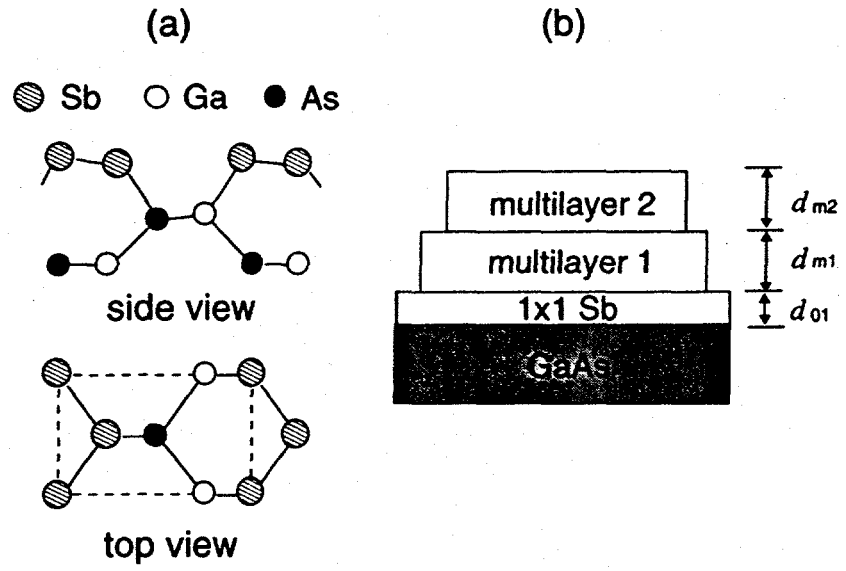

Figure 8: (a) Schematic diagrams of the side and top views of the epitaxial continued layer structure model for the 1ML-Sb/GaAs(110)-(1x1) system. (b) Schematic cross-section view depicting Sb multilayers on the GaAs(110) substrate.

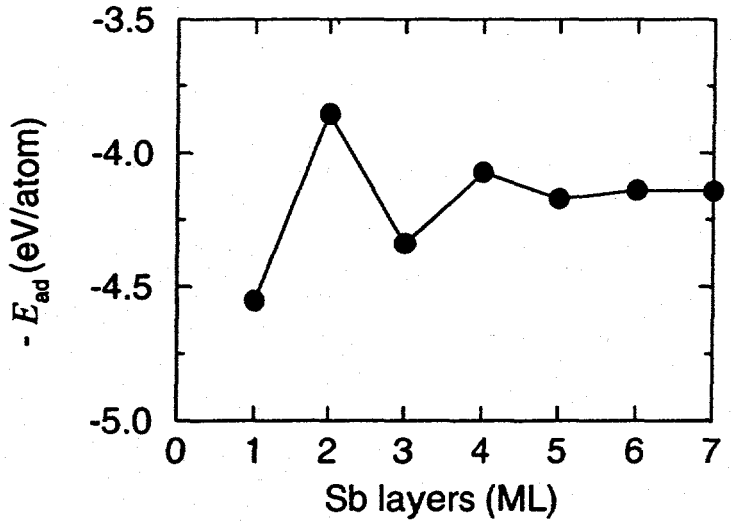

Figure 9: Negative adsorption energy as a function of the Sb coverage.

physical reasons for the existence of the oscillatory nonmetal-metal transitions, discuss the results in comparison with existing experiments, and suggest new ways to test some of the unique predictions made here.

In our calculations, we use norm-conserving separable pseudopotentials[38,39] together with the density-functional theory within the local-density approximation[40,41] (LDA). Partial-core corrections are included in the pseudopotentials of Ga[42]. We model the Sb/GaAs(110) system by a periodic slab geometry. Each slab contains seven GaAs substrate layers and a certain Sb overlayer on each side of the slab. The vacuum region between such slabs has a thickness of about 10 Å. The Sb overlayer is modeled by the so-called epitaxial continued layer structure[35,36,37], where the Sb atoms grow epitaxially in a form of zig-zag chains in the $[1\bar{1}0]$ direction on a nearly bulk-like GaAs(110) substrate (see Fig. 8). To optimize the atomic structure, atoms in the overlayer and the substrate are relaxed along the calculated forces until the remaining forces are all within 6 mRy/Å. We employ a plane-wave basis with an energy cutoff of 10 Ry and take a uniform grid of 24 **k** points within the (1×1) surface Brillouin-zone. The calculation scheme and its previous application to the Sb monolayer on GaAs(110) are described in detail elsewhere[37].

In order to examine the relative stability of Sb adsorption on GaAs(110) with increasing Sb coverage, we calculate the adsorption energy ($E_{\rm ad}$) per Sb atom from

$$E_{\rm ad} = (E(n-1) + 4E^a_{\rm Sb} - E(n))/4 \qquad (11)$$

where $E(n-1)$ and $E(n)$ is the total energy per unit cell for a slab with the Sb coverage, L, equal to $(n-1)$ and n ML, respectively, and $E^a_{\rm Sb}$ is the total energy of a free Sb atom. In the case of $n = 1$, $E(n-1)$ corresponds to the total energy of the clean GaAs(110) surface. The negative of the adsorption energy with respect to the Sb coverage is plotted in Fig. 9, showing strongly oscillatory size effects: The adsorption energies at $L = 1$, 3, and 5 ML are larger than those at 2 and 4 ML. This energetic information indicates that, the first Sb monolayer, at which the adsorption energy is the largest, binds most strongly to the GaAs substrate. A flat film at $L = 3$ or 5 ML is locally stable, but a flat film at 2 or 4 ML is unstable against roughening. Therefore, one expects Sb growth on GaAs(110) to follow the $(1 + M)$ mode, with $M = 2$. This finding qualitatively explains the experimentally observed $(1 + M)$ growth mode in this system. However, we note that on a quantitative level earlier experiments suggested M to be 3, estimated by using the constant bulk interlayer spacing for the Sb thin films[32,33]. As shown below, this discrepancy can be resolved by considering the large deviations of the interlayer spacings in the Sb thin films from the bulk value. Figure 9 also shows that the adsorption energy changes little above 6 ML of Sb: therefore, the double layer growth mode will no longer be favored at such higher coverages.

In Table 1, we summarize the calculated interlayer spacings of the Sb overlayers. It is worth to emphasize the following aspects. (i) the topmost Sb-Sb interlayer spacing varies with the film thickness in an oscillatory way, taking the values of 2.94, 2.77, 2.88, 2.79, and 2.81 Å as L increases from 2 to 6 ML. After 6 ML the oscillation disappears. Such variations in the topmost interlayer spacing should be observable, for example by measuring the height of sizeable monolayer-high islands formed at the growth front, as reported in a recent experimental study of Pb/Ge(100)[43]. (ii) for a given coverage, the interlayer spacing also oscillates from layer to layer.

The present results for the heights of double Sb layers ($d_{\rm m1}$ and $d_{\rm m2}$ in Fig. 8) are

Table 1: Calculated interlayer spacings (in Å) for the Sb overlayers on GaAs(110).

	d_{01}	d_{12}	d_{23}	d_{34}	d_{45}	d_{56}	d_{67}
1 ML	2.39						
2 ML	2.54	2.94					
3 ML	2.41	3.44	2.77				
4 ML	2.44	3.28	2.99	2.88			
5 ML	2.43	3.25	2.86	3.16	2.79		
6 ML	2.44	3.28	2.87	2.97	3.02	2.81	
7 ML	2.43	3.24	2.89	3.00	2.94	3.08	2.81

given in Table 2 together with those from experiments[32,33]. The values of $d_{m1} = 6.2$ Å and $d_{m2} = 6.0$ Å are in good agreement with the STM measurements of Shih, Feenstra, and Mårtensson [32] ($d_{m1} = 6.0 \pm 0.5$ Å and $d_{m2} = 6.0 \pm 0.5$ Å) and Patrin *et al.* [33] ($d_{m1} = 6.4 \pm 0.5$ Å and $d_{m2} = 6.4 \pm 0.5$ Å). However, both STM studies estimated the coverages of the first and the second multilayers to be 4 ML and 7 ML, respectively, by using the bulk interlayer spacing of about 2 Å. Our calculations show that the interlayer spacings in the thin Sb overlayers are significantly larger than the bulk value (see Table 1), a prediction to be confirmed in future experiments.

The oscillatory behavior of the interlayer spacing is a consequence of the quantum size effect. The electronic density in the quantum well has an oscillatory position dependence in the growth direction. It is natural to expect similar adjustment of the ions to minimize the electron-ion interaction energy[13]. Here we only like to emphasize the observation that the amplitude of oscillation is particularly large at $L = 3$ ML, when the system is in the nonmetallic state (see below). This can be explained qualitatively by the fact that in the nonmetallic state the charge density fluctuation is associated with one-dimensional screening, while in the metallic state the magnitude of the fluctuation associated with three-dimensional screening is smaller.

We have also obtained the band structures of the system at different Sb coverages, with those at 1 and 2 ML shown in Fig. 10. There are four subbands in the bulk gap at $L = 1$ ML[35,36]; the lower two subbands are fully occupied, and the higher ones are empty. Thus the 1-ML Sb overlayer is nonmetallic with a band gap of 0.9 eV. The 2-ML Sb overlayer has two additional subbands in the bulk gap, which overlap across the Fermi energy, leading to a metallic state. Surprisingly, these overlapping subbands appear oscillatorily with increasing Sb thickness: They disappear at 3 ML and reappear at 4 ML. As a result, the 3-ML Sb overlayer has a band gap of 0.1 eV, and the 4-ML Sb overlayer shows a metallic state. Above $L = 5$ ML the system is always metallic. The calculated band gap with respect to the Sb coverage is summarized in Fig. 11. It is well known that the LDA calculation underestimates the band gap. For example, the experimental band gap at 1 ML is about 1.3 eV[32,33], larger than the calculated value of 0.9 eV. Therefore, we expect that the real band gap at 3 ML is also larger than the present LDA value of 0.1 eV. Because the 2- and 4-ML Sb overlayers show metallic behavior with the presence of the two overlapping subbands at the Fermi energy, they are energetically unstable compared to the 1- and 3-ML Sb overlayers, consistent with the results shown in Fig. 9.

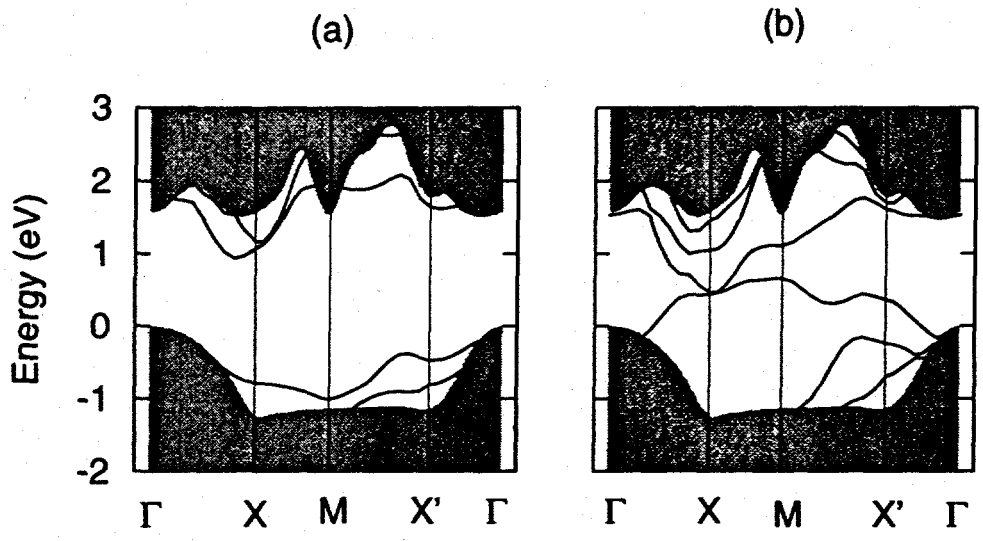

Figure 10: Surface band structures of Sb/GaAs(110)-(1x1) at two Sb coverages: (a) 1 ML; (b) 2 ML.

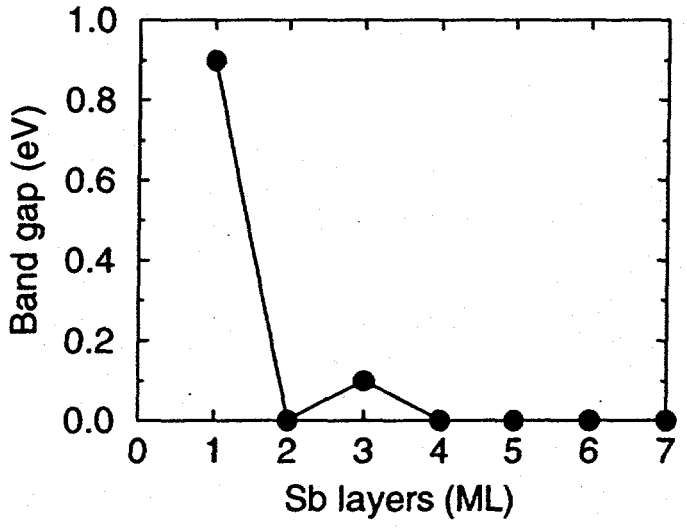

Figure 11: Band gap as a function of the Sb coverage.

Table 2: Calculated heights (in Å) of Sb multilayers in comparison with experimental results. For the denotations of d_{m1} and d_{m2}, see Fig. 8. The interlayer spacing between the Sb layer and the GaAs substrate (d_{01}) is given for comparison.

	d_{01}	d_{m1}	d_{m2}
present study	2.4	6.2	6.0
STM I[32]	2.5	6.0 ± 0.5	6.0 ± 0.5
STM II[33]	2.5	6.4 ± 0.5	6.4 ± 0.5

It is remarkable that the Sb overlayers on GaAs(110) show oscillatory nonmetal-metal transitions. For metal overlayers on semiconductor substrates, the typical picture for nonmetal-metal transition is as follows[44]: The overlayer is nonmetallic if the coverage is too low, becomes metallic at some critical coverage, and is expected to be more metallic if additional layers of metal are added. However, in the present study we find that a metallic overlayer at $L = 2$ ML will turn into a nonmetallic state if one more layer of Sb is added.

The unusual oscillatory nonmetal-metal transitions can be explained by the classic Wilson rule[45], generalized to the present case, and constrained by the quantum size effect of the thin film. Because the dangling bonds of the topmost Sb layer atoms is fully occupied, we can regard our quantum well to really start at $L = 2$ ML. At $L \geq 2$ ML, because each Sb atom is tetrahedrally bonded in the (1x1) structure, each unit cell of a given Sb layer contains two nearly equivalent "free" electrons. Therefore, the total number of such electrons per unit cell of the thin film is always an even number, $2n$, with $n = 1, 2, 3, \ldots$ for $L = 2, 3, 4, \ldots$ ML. On the other hand, each additional Sb layer also contributes two overlapping subbands, due to the confinement in the vertical direction. For small enough film thicknesses at which different subbands originated from different Sb layers do not overlap in energy, we expect metal-nonmetal transitions according to a generalized Wilson rule: metal for odd n and nonmetal for even n. Therefore, we have a metallic system at $L = 2$ ML, a nonmetal at 3 ML, and a metal again at 4 ML. This oscillatory behavior will stop, however, if the film is above a critical thickness where the spacing between the subbands contributed by neighboring layers becomes smaller than the width of the subbands, because then the different subbands overlap in energy and only the metallic state prevails. Below the critical thickness, we expect that the gap between the filled and empty subbands of the nonmetallic state decreases with the film thickness, as shown in Fig. 11. Based on the above picture, we further infer that oscillatory nonmetal-metal transitions should *not* be expected in alkali metal films on semiconductors, because the subbands associated with those simple metals are typically very broad. On the other hand, for systems of metal overlayers with flatter subbands, oscillatory nonmetal-metal transitions can persist to even higher film coverages. At present, we are developing a phenomenological description of the oscillatory metal-nonmetal transitions aimed to explore the phase space in which such oscillations persist to higher film thicknesses.

5 Summary and discussions

This paper is centered around the presentation of the novel concept of "electronic growth". This concept contains three essential ingredients: quantum confinement, which

leads to a repulsive force working to stabilize metal films of any thickness: charge spilling, which leads to an attractive force working to destabilize particularly thinner films; and interface-induced Friedel oscillations, which may introduce additional modulations in the effective long-ranged interaction potential. The theory provides new understanding on many existing observations in previous studies of ultrathin metallic overlayer growth on semiconductor substrates. For example, the observation of critical thicknesses for smooth growth of Ag on GaAs, GaP, and GaSb [8,9,10], and the fact that only the first layer of alkali metals can grow smoothly on GaAs [14] provide strong evidences for the validity of the theory. We also suspect that the peculiar features frequently observed during the growth of the first few monolayers of metals on semiconductors [46] may have their origin tied to the existence or absence of the critical/magic thicknesses in such systems. More importantly, one can devise new experiments to test systematically the unique predictions made here. In doing so, one should bear in mind two optimal conditions: the overlayer metal should be soft (as it is the case for Ag), so as to minimize the effect of the strain energy; and there should be minimal intermixing at the interface, so as to maximize the effect of a sharp interface. For many systems, the second requirement demands sufficiently low growth temperatures. Lower-temperature deposition is especially required to test the existence of the magic and critical thicknesses shown in Types C and D of Fig. 3, because one typically needs to have an initial film close to the stable flat film configuration. For systems in which such critical/magic thicknesses do exist, the morphology of the metallic overlayers can be controlled down to the atomic scale. It should also be possible to tune the values of the critical/magic thicknesses by tuning the band alignment. Therefore, the electronic growth mechanism in principle provides an important tool for quantum engineering of metallic thin films on semiconductor substrates.

We have also shown that suitable long-range interactions can stabilize epilayers against stresses. Substantial work is needed to study long-range interaction of various physical origins. In particular, forces prevalent in colloids and liquid films, such as that due to electrical double-layers, should be examined to determine their relevance to solid films. Long range interactions may play significant roles in other phenomena in nanostructures. It is hoped that experiments will soon succeed in confirming the predictions made here, and independently measuring the excess energy of solid films.

On a more rigorous level, our first-principles calculations have shown that, in the model growth system of Sb/GaAs(110), quantum size effects can prevail in several dramatic ways. The adsorption energy per layer has been found to oscillate with the overlayer thickness, making flat films at 1, 3, and 5 ML coverages magically stable, while films at 2 and 4 ML unstable. This finding qualitatively explains the $(1 + M)$ growth mode observed in previous experiments, and calls for more precise determination of M in future experiments. For films at different thicknesses, there exist strong oscillations in the topmost interlayer spacings; and for a film of a given coverage, the interlayer spacing within the film should also oscillate from layer to layer. There should also exist oscillatory nonmetal-metal transitions as the film thickness increases, a prediction to be confirmed in future experiments (for example by locally probing the band gaps using the scanning tunneling spectroscopy). All these oscillatory properties, in the stability, interlayer spacing, and transport, are correlated at the fundamental level.

Finally, we mention that the effects of quantum confinement, charge spilling, and

Friedel oscillations are not limited to the cases of three-dimensional film growth. For example, in a recent study, these similar phenomena were found to play important roles in the formation of two-dimensional metal islands on surfaces, leading to the existence of magic length scales in metal submonolayer epitaxy[17]. We expect that the present line of study will stimulate intensive research activities, both experimental and theoretical, to further explore the importance and fascinating manifestations of quantum size effects in various systems of reduced dimensions.

We gratefully acknowledge Myung-Ho Kang, Jerry Mahan, Ward Plummer, Jerry Tersoff, John Weaver, and Hanno Weitering for helpful and informative discussions. This research was supported by Oak Ridge National Laboratory managed by Lockheed Martin Energy Research Corp. for the U.S. Department of Energy under Contract No. DE-AC05-96OR22464, and by the National Science Foundation (grant numbers MSS-9258115 and DMR-9705406).

References

1. See, for example, articles in Physics of Low-Dimensional Semiconductor Structures. P. Butcher, N. H. March, M. P. Tosi, Eds. (Plenum, New York, 1992).
2. J. H. van der Merwe, J. Appl. Phys. **34**, 117 (1963); *ibid.*, p123. J. W. Matthews and A. E. Blakeslee, J. Cryst. Growth **29**, 273 (1975); *ibid.* **32**, 265 (1976). J. Tersoff, Appl. Phys. Lett. **62**, 693 (1993). D. E. Jesson, K. M. Chen, S. J. Pennycook, T. Thundat, R. J. Warmack, Science **268**, 1161 (1995).
3. R. J. Asaro and W. A. Tiller, Metall. Trans. **3**, 1789 (1972). M. A. Grinfeld, J. Nonlinear Sci. **3**, 35 (1983). D. J. Srolovitz, Acta Metall. **37**, 621 (1989). B. J. Spencer, P. W. Voorhees, S. H. Davis, Phys. Rev. Lett. **67**, 3696 (1991). J. Tersoff and F. K. LeGoues, *ibid.* **72**, 3570 (1994).
4. See, for example, the review articles in the special issue on Heteroepitaxy and Strain, MRS Bulltin **22** (No. 4) (1996).
5. J. Villain, J. Phys. I (France) **1**, 19 (1991). J. A. Stroscio, D. T. Pierce, M. D. Stiles, A. Zangwill, L. M. Sander, Phys. Rev. Lett. **75**, 4246 (1995).
6. For a review on various growth mechanisms based on atomistic processes, see Z. Y. Zhang and M. G. Lagally, Science **276**, 377 (1997).
7. B. M. Trafas, Y.-N. Yang, R. L. Siefert, J. H. Weaver, Phys. Rev. B **43**, 14107 (1991).
8. A. R. Smith, K.-J. Chao, Q. Niu, and C. K. Shih, Science **273**, 226 (1996).
9. G. Neuhold, L. Bartels, J. J. Paggel, K. Horn, Surf. Sci. **376**, 1 (1997).
10. K.-J. Chao, Q. Niu, Z. Y. Zhang, C.K. Shih, (to be published).
11. Z. Y. Zhang, Q. Niu, and C.-K. Shih, Phys. Rev. Lett. (submitted, 1997).
12. R. C. Jaklevic, J. Lambe, M. Mikkor, and W. C. Vassell, Phys. Rev. Lett. **26**, 89 (1971). M. Jalochowski and E. Bauer, Phys. Rev. B **38**, 5272 (1988). T. Miller, A. Samsavar, G. E. Franklin, T. C. Chiang, Phys. Rev. Lett. **61**, 1404 (1988). B. J. Hinch, C. Koziol, J. P. Toennies, and G. Zhang, Europhys. Lett. **10**, 341 (1989). E.Ortega and F. J. Himpsel, Phys. Rev. Lett. **69**, 844 (1992). D. A. Evans, M. Alonso, R. Cimino, K. Horn, Phys. Rev. Lett. **70**, 3483 (1993).
13. F. K. Schulte, Surf. Sci. **55**, 427 (1976). P. J. Feibelman, Phys. Rev. B **27**, 1991 (1983). P. J. Feibelman and D. R. Hamann, Phys. Rev. B **29**, 6463 (1984). I. P.

Batra *et al.*, Phys. Rev. B **34**, 8246 (1986). N. Trivedi and N. Ashcroft, Phys. Rev. B **38**, 12298 (1988).
14. N. J. DiNardo, T. M. Wong, and E. W. Plummer, Phys. Rev. Lett. **65**, 2177 (1990). L. J. Whitman, J. A. Stroscio, R. A. Dragoset, and R. J. Celotta, Phys. Rev. Lett. **66**, 1338 (1991). O. Pankratov and M. Scheffler, Phys. Rev. Lett. **70**, 351 (1993).
15. Z. G. Suo and Z. Y. Zhang, Phys. Rev. Lett. (submitted, 1997).
16. J.-H. Cho, Q. Niu, and Z. Y. Zhang, Phys. Rev. Lett. (submitted, 1997).
17. K.-j. Jin, G. D. Mahan, H. Metiu, and Z. Y. Zhang, Phys. Rev. Lett. (in press) (1998).
18. W. D. Knight, K. Clemenger, W. A. de Heer, W. A. Saunders, M. Y. Chou, M. L. Cohen, Phys. Rev. Lett. **52**, 2141 (1984).
19. J. Tersoff, Phys. Rev. Lett. **52**, 465 (1984).
20. S. G. Louie, J. R. Chelikowsky, and M. L. Cohen, Phys. Rev. B **15**, 154 (1977).
21. N. W. Ashcroft and N. D. Mermin, Solid State Physics (Saunders, Philadelphia, 1976).
22. A. M. Cowley and S. M. Sze, J. Appl. Phys. **36**, 3212 (1965).
23. S. B. Zhang and A. Zunger, Phys. Rev. B **53**, 1343 (1997).
24. D. J. Eaglesham and M. Cerullo, Phys. Rev. Lett. **64**, 1943 (1990). Y.-M. Mo, D. E. Savage, B. S. Swartzentruber, M. G. Lagally, Phys. Rev. Lett. **65**, 1020 (1990). F. K. LeGoues, M. Copel, and R. M. Tromp, Phys. Rev. B **42**, 11690 (1990). M. Asai, H. Ueba, and C. Tatsuyama, J. Appl. Phys. **58**, 2577 (1985).
25. W. J. Schaffer et al., J. Vac. Sci. Technol. B **1**, 688 (1983). C. W. Snyder, B. G. Orr, and H. Munekata, Appl. Phys. Lett. **62**, 46 (1992). D. Leonard, M. Krishnamurthy, S. Fafard, J. L. Merz, and P. M. Petroff, J. Vac. Sci. Technol. B **12**, 1063 (1994). R. Leon, S. Fafard, D. Leonard, J.L. Merz, and P.M. Petroff, Appl. Phys. Lett. **67**, 521 (1995). Q. K. Xue and T. Sakurai, (preprint, 1997). S.R. Forrest, Chem. Rev. **97**, 1793 (1997).
26. M. Grinfeld, Sov. Phys. Dokl. **31**, 831 (1986). H. Gao, Int. J. Solids Structure **28**, 703 (1991). L. B. Freund and F. Jonsdottir, J. Mech. Phys. Solids **41**, 1245 (1993).
27. Here we use the simplest version of the model to compare the relative magnitudes of various thermodynamic forces. The effect of surface tension anisotropy can be important. See J. Tersoff and F. K. LeGoues, Phys. Rev. Lett. **72**, 3570 (1994); D. E. Jesson, K.M. Chen, S. J. Pennycook, T. Thundat, R. J. Warmack, Phys. Rev. Lett. **77**, 1330 (1996). A quantitative comparison of effects of surface tension anisotropy and long-range interaction is beyond the scope of this paper.
28. C.-H. Chiu and H. Gao, Mat. Res. Soc. Proc. **356**, 33 (1995).
29. P. M. Petroff, and S. P. DenBaars, Superlattices and Microstructures **15**, 15 (1994).
30. A. Grossmann, W. Erley, J. Hannon, and H. Ibach, Phys. Rev. Lett. **77**, 127 (1996).
31. R. Strümpler and H. Lüth, Surf. Sci. **182**, 545 (1987).
32. C. K. Shih, R. M. Feenstra, and P. Mårtensson, J. Vac. Sci. Technol. A **8**, 3379 (1990).
33. J. C. Patrin, Y. Z. Li, M. Chander, and J. H. Weaver, Phys. Rev. B **46**, 10221 (1992).

34. C. B. Duke *et al.*, Phys. Rev. B **26**, 803 (1982). P. Mårtensson and R. M. Feenstra, Phys. Rev. B **39**, 7744 (1989). W. K. Ford *et al.*, Phys. Rev. B **42**, 8952 (1990). M. G. Betti *et al.*, Phys. Rev. B **50**, 14336 (1994). H. Ascolani *et al.*, Phys. Rev. Lett. **78**, 2604 (1997).
35. G. P. Srivastava, Phys. Rev. B **46**, 7300 (1992); *ibid.*, **47**, 16616 (1993).
36. W. G. Schmidt, B. Wenzien, and F. Bechstedt, Phys. Rev. B **49**, 4731 (1994).
37. J.-H. Cho, Z. Y. Zhang, S. H. Lee, and M. H. Kang, Phys. Rev. B **57**, 1352 (1998).
38. L. Kleinman and D. M. Bylander, Phys. Rev. Lett. **48**, 1425 (1982).
39. N. Troullier and J. L. Martins, Phys. Rev. B **43**, 1993 (1991).
40. P. Hohenberg and W. Kohn, Phys. Rev. **136**, B864 (1964); W. Kohn and L. J. Sham, Phys. Rev. **140**, A1133 (1965).
41. D. M. Ceperley and B. J. Alder, Phys. Rev. Lett. **45**, 566 (1980). J. P. Perdew and A. Zunger, Phys. Rev. B **23**, 5048 (1981).
42. S. G. Louie, S. Froyen, and M. L. Cohen, Phys. Rev. B **26**, 1738 (1982).
43. A. Crottini, D. Cvetko, L. Floreano, R. Gotter, A. Morgante, and F. Tommasini, Phys. Rev. Lett. **79**, 1527 (1997).
44. E. W. Plummer and P. A. Dowben, Progress in Surface Science, **42**, 201 (1993). P. A. Dowben, Rev. Modern Phys. (to appear).
45. A. H. Wilson, Proc. Roy. Soc. A **133**, 458 (1931).
46. V. A. Grazhulis, Prog. Surf. Sci. **36**, 89 (1991). M. Jalochowski, H. Knoppe, G. Lilienkamp, E. Bauer, Phys. Rev. B **46**, 4693 (1992). E.T. I. M. Bootsma and T. Hibma, Surf. Sci. **287/288**, 921 (1993).